



SIZE EVOLUTION OF A SOLUBLE AEROSOL PARTICLE IN AIR

Y.L. Kuznetsova

Institute of Continuous Media Mechanics UB RAS, Perm, Russian Federation

The mechanisms responsible for hygroscopic growth (or reduction) in the size of water-soluble aerosol particles have a significant effect on the dynamics of coagulation and sedimentation processes in aerosol systems. By now, there is a large amount of experimental and theoretical works devoted to the study of hygroscopic growth and decrease in the size of particles of various chemical nature. Along with comprehensive multilayer models of aerosol particle growth, the models based on the modification of the Maxwell equation for condensation and evaporation of droplets are widely used. Such models can take into account temperature effects, the influence of the surface curvature of the particle, and the presence of soluble substances in it. The paper proposes a mathematical model of the evolution of the size of water-soluble aerosol particles that, along with the listed effects, takes into account the change in the size of the undissolved particle core. This approach makes it possible to simulate all the stages of hygroscopic change in the particle size: from the transformation of a crystal core into a drop to its subsequent growth, as well as in the opposite direction - from the evaporation of a drop to the formation of a crystal. Based on the proposed model, various scenarios for changing the state of a particle on its initial degree of solubility and the relative humidity of the air were studied. It is shown that the predictions of the model are qualitatively and quantitatively consistent with the experimental data on the evolution of the particle size of sodium chloride in the modes of humidification and drying, as well as with the results of measurements of particle sizes in equilibrium state with variations in the relative humidity of the air. The developed model can be used to solve various fundamental and applied problems of the dynamics of water-soluble aerosol systems.

Key words: water-soluble aerosol particles, hygroscopic particle growth model, aerosol particle dissolution and evaporation, computational experiment, numerical solution

1. Introduction

The study of the interaction of aerosol particles with air moisture is of great importance in solving many applied problems: determining the nature of the spread of environmental pollution, evaluating the pharmaceutical effects of inhalation treatment, designing mine ventilation systems for salt mines, etc. When substances are dissolved in humid air, in contrast to liquids, hydrated molecules (ions) of the substance remain on the surface of the particle and form a solution layer on it, the concentration of which changes during the dissolution process. In this case, an increase in the size and mass of particles occurs, which in turn affects the rate of their coagulation and sedimentation.

To describe the hygroscopic properties of substances, absorption isotherms are mainly used, which show the dependence of the equilibrium size of a water-soluble aerosol particle on the relative humidity of the air [1]. The typical pattern of the particle absorption isotherm for pure NaCl, pre-dried crystals with an initial effective diameter of 99 nm, is illustrated in Fig. 1 (taken from [2]). The experimental investigations have been performed using a hygroscopicity tandem differential mobility analyzer (H-TDMA) at a fixed ambient temperature of 298K. An equilibrium particle diameter has been measured at various fixed values of relative air humidity.

The process of hydration (or dehydration) can be divided into several areas on the experimental curves (Fig. 1. As the relative humidity of the air increases from zero (area I), the adsorption process occurs on the surface of the soluble particle but the initial radius of the crystal practically does not change. When the relative humidity reaches a certain critical value - the hygroscopic point or DRH (Deliquescence Relative Humidity) - the crystal begins to be covered with a water film and partially dissolves in it, forming a saturated solution. Thus, in area II, at a constant relative humidity of the air, the radius of the particle, which includes a crystal core and a solution on the surface, increases monotonically until complete dissolution. As a result, a drop is formed, the radius of which can be several times greater than the radius of a dry crystal. A further rise in the relative humidity leads to an increase in the equilibrium radius of a completely dissolved particle (area III). As the relative humidity of the air decreases, the droplet radius begins to decrease in accordance with the area of increasing (area II). However, at the relative humidity of DRH dissolution, no solid crystal appears inside the droplet. The value of relative air humidity at which the reverse phase transition ERH (Efflorescence Relative Humidity) occurs is lower than DRH. This is due to the fact that if there are no heterogeneous additives, then the reverse phase transition occurs as a result of homogeneous nucleation. For the formation of a nucleation

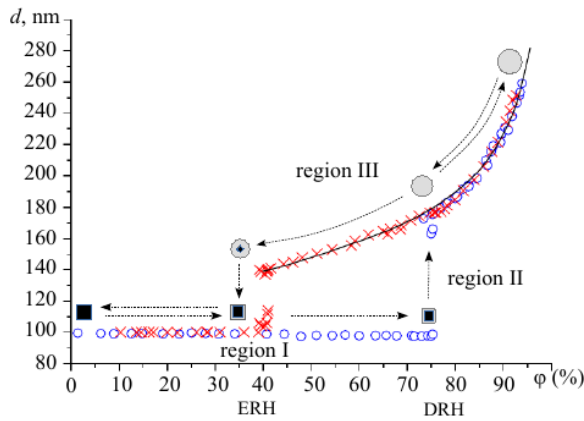


Fig. 1. The experimentally observed evolution of the effective diameter of NaCl particles for an increase (circles ○) and a decrease (crosses ×) in the relative humidity [2]. Theoretical description of the process using the Köhler equation (solid black line) [3].

Various forms of this equation are proposed, which make it possible to take into account the influence of the chemical composition and surface tension of a particle on its hygroscopic properties [6-8].

For many applied problems, in addition to the equilibrium state, it is required to determine the times of dissolution, evaporation, and crystallization of particles, as well as the kinetics of these processes. The first works on the theoretical description of the hygroscopic increase (decrease) in particle diameter were based on the Maxwell's equation for the condensation and evaporation on (from) the surface of a spherical drop that is fixed in a homogeneous medium:

$$\frac{dm}{dt} = \frac{4\pi r_* D_f M_1}{R_g T} (p_\infty - p_*) \quad (1)$$

where m , r_* — mass and radius of the drop, M_1 — molar mass of water, R_g — universal gas constant, D_f — vapor diffusion coefficient, T — drop and ambient medium temperature, p_* and p_∞ — vapor pressure at the surface of the diluting droplet and atmospheric pressure.

Models based on modifications of the Maxwell equation by specifying various options for the relationship between vapor pressure on the surface of a particle and its size, as well as by taking into account thermal effects (separating temperatures of the particle T_* and the surrounding air T_∞), are widely used. Such models make it possible to describe the characteristic features of the evaporation kinetics of small particles and the nonlinearity of the dissolution process associated with a change in the solution concentration in a drop, as well as take into account the change in particle temperature caused by the condensation (evaporation) of water molecules [9–11]. However, when describing the evolution of the particle size using such models, in most cases, for example, in [9], a transition is made from differentiation with respect to mass to a derivative with respect to the radius (diameter) of the particle in the form:

$$r_* \frac{dr_*}{dt} = \frac{D_f M_1}{R_g \rho} \left[\frac{p_\infty}{T_\infty} - \frac{p_*}{T_*} \right], \quad (2)$$

assuming, thereby, that the density of the particle is constant $\rho = \text{const}$. According to the author of this article, such a transition is incorrect due to the fact that the density of the particle changes during the dissolution process.

In addition, since such models do not take into account the influence of the undissolved nucleus on the solution concentration at the particle surface, they are not able to represent all stages of increase (decrease) in the particle diameter. In some works, for example, in [11], in order to reconstruct the hygroscopic growth of a particle, the equations are artificially divided into stages before and after the complete dissolution of the crystalline substance of the particle.

core of a crystal phase, it is necessary to overcome the energy barrier. This is possible when the solution becomes supersaturated with respect to the solid phase in the area of the metastable state of the particle. In practice, this effect manifests itself in the form of a hysteresis of the hygroscopic properties of the particle, i.e.

in a mismatch between the curves of hydration and dehydration at relative air humidity below the DRH value.

The explanation of the dependences presented above is in full agreement with the thermodynamic theory. Area I is determined by solving the problem of the pressure of saturated vapor over a drop of a solution that includes a solid soluble nucleus [4]. Area II can be calculated from the condition of thermodynamic stability of a solution drop covering a soluble nucleus [5]. In the theoretical description of area III, the Köhler equation is commonly used [3].

At present, multilayer kinetic models, such as [12,13] and others, are extensively used, in which, due to the division of the volume of a particle into layers, a clear separation of various physical and thermodynamic processes on each layer, as well as setting the mutual influence of processes on each other, it is possible to describe the complex kinetics of dissolution of particles, taking into account many factors. Such models are widely used to characterize the behavior of multicomponent aerosol particles containing both soluble and insoluble chemically active substances of organic and inorganic nature. The most complete kinetic model of this type is the KM-GAP model [14], which incorporates the multilayer principle and, in addition to the transport properties of molecules, considers chemical reactions between particle components. This model can be aimed at studying the evolution of atmospheric aerosols. The most complete review of the current state of atmospheric aerosol thermodynamics and modeling of their mass transfer can be found in [15].

The purpose of this work is:

- to develop an improved model, based on the Maxwell equation, for the evolution of the size of a particle in a water vapor medium, including phase transitions of dissolution and crystallization;
- to verify models based on known experimental data on the hygroscopic evolution of sodium chloride particle size;
- to estimate the magnitude of the particle density change in the process of dissolution.

2. Mathematical model of particle size evolution

Let us consider air as a mixture of non-condensable passive gas and condensable water vapor, with relative humidity $\varphi = p_\infty / p_n(T_\infty)$, where p_∞ — vapor pressure away from particle, and $p_n(T_\infty)$ — equilibrium pressure of saturated vapor at a given temperature. A water-soluble aerosol particle placed in this air mixture can increase or decrease its size depending on the ratio of vapor pressure above the surface of the particle $p_* \equiv p(r_*)$ and away from it p_∞ .

To simplify calculations, the particle is considered to be spherically symmetric with the effective radius r_* (Fig. 2). Let us denote the total number of molecules in a particle as $n = n_1 + n_2$, while n_1 — the number of water molecules, and a $n_2 = n_{2k} + n_{2d} = \text{const}$ — where n_{2k} , n_{2d} - the number of matter molecules that are in a crystalline and dissolved state, respectively.

Using the approximation of a volume additivity, i.e. assuming that the total volume of a dissolved particle is equal to the sum of the volumes of a dry particle and absorbed water [8], we establish a relationship between the particle radius and the number of water and solute molecules:

$$V = 4\pi r_*^3 / 3 = n_1 v_1 + n_2 v_2, \quad (3)$$

where v_1 , v_2 — molecules volumes of water and matter.

The initial state of a particle is given by its radius r_0 and the mole fraction of water in the particle $x_{10} = n_{10} / n$, where n_{10} - the number of water molecules in the particle at the initial moment. Then:

$$n_2 = \frac{4\pi}{3} r_0^3 \left/ \left(\frac{x_{10}}{1-x_{10}} v_1 + v_2 \right) \right., \quad n_{10} = \frac{x_{10} n_2}{(1-x_{10})}. \quad (4)$$

As mentioned above, when a dry particle is placed in humid air, the process of adsorption of water molecules on its surface first occurs, therefore, to determine the number of dissolved molecules of the initial dry matter at the initial time n_{2d0} , the value of n_{10} is compared with the equilibrium number of water molecules that can be adsorbed on the surface of the particle at a given relative air humidity A_φ . The dependence of A_φ on the relative air humidity was set by the equation of the polymolecular (multilayer) BET adsorption isotherm [16]:

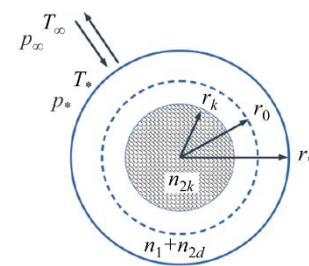


Fig. 2. Particle model.

$$A_\varphi \equiv A(\varphi) = A_n \frac{c\varphi}{(1-\varphi)(1+(c-1)\varphi)}. \quad (5)$$

Here: c is the ratio of the adsorption equilibrium constants in the first layer to the condensation constant, which, according to [17] for the adsorption of water molecules on NaCl surface $c = 1,5$; parameter A_n is equal to the number of water molecules required to create a monolayer around a dry particle and is determined from the relationship:

$$A_n = \frac{16}{d_1^2} \left(\frac{3n_2v_2}{4\pi} \right)^{2/3}, \quad (6)$$

where $y = x$ — water molecule diameter.

If the condition R^2 is met, all the molecules of the dissolved matter are in the crystalline state, i.e.

$$T = 299,15 \quad \text{and} \quad n_{2k0} = n_2. \quad (7)$$

If this condition is not met, then the number of dissolved molecules of the matter is determined by the relation:

$$n_{2d0} = n_{10}K(M_1/M_2), \quad n_{2k0} = n_2 - n_{2d0}. \quad (8)$$

where M_1, M_2 - molar masses of water and matter, K - solubility of a matter in water (for sodium chloride $K_{\text{NaCl}} \approx 36\text{r}/100\text{r}$ water at a temperature 298,15K). If $n_{10}K(M_1/M_2) > n_2$, then the particle is considered to be completely dissolved, which means:

$$n_{2d0} = n_2, \quad n_{2k0} = 0. \quad (9)$$

The change in the number of water molecules in a particle occurs due to their flow through the surface of the particle. Assuming the flow to be diffusion related to the difference in vapor pressures far from the particle and on its surface, the mass balance equation is described by the Maxwell equation, which, taking into account thermal effects and substitution $m = \rho_1v_1n_1 + \rho_2v_2n_2$, where $n_2 = \text{const}$, takes the form:

$$\frac{dn_1}{dt} = \frac{4\pi r_* D_f p_n(T_\infty)}{k_b} \left(\frac{\varphi}{T_\infty} - \frac{1}{T_*} \frac{p_*(T_\infty)}{p_n(T_\infty)} \right), \quad (10)$$

where D_f — diffusion coefficient of water molecules in air, k_b — Boltzmann's constant, T_* , T_∞ — vapor temperature at the particle surface and away from it. The particle radius is determined from the relation (3):

$$r_* = \left[\frac{3}{4\pi} (n_1v_1 + n_2v_2) \right]^{1/3}. \quad (11)$$

As in [9], when calculating the pressure of saturated vapor on the particle surface, the following is taken into account:

– dependence of its value on temperature, in the form of a modification of the Clausius-Clapeyron equation:

$$p_*(T_*) = p_n(T_\infty) \exp \left[\frac{LM_1}{R_g} \left(\frac{1}{T_\infty} - \frac{1}{T_*} \right) \right], \quad (12)$$

where L — specific heat of vaporization/condensation;

– pressure increase due to particle surface curvature (Thomson formula):

$$p_*(T_*) = p_n(T_*) \exp\left(\frac{2\sigma_1 v_1}{r_* k_b T_*}\right), \quad (13)$$

where σ_1 — surface tension of water;

– decrease in its value due to the presence of soluble compounds in the particle, which is characterized by the activity of water in solution a_w :

$$p_*(T_*) = p_n(T_*) a_w. \quad (14)$$

The application of the equation (14) requires specifying the dependence of water activity on the concentration of the matter dissolved in it. Currently, several variants of such ratios are known in the literature. For inorganic salts, equations based on the polynomial functions approximation of experimental measurements results for a given matter have become widespread [18-20]. In this paper, we use a cubic equation for the mass fraction of a solute matter in a particle Y , built on the basis of water activity measurements for sodium chloride particles [18]:

$$a_w = 1 - 5,5741 \times 10^{-3} Y - 5,8805 \times 10^{-5} Y^2 - 3,2005 \times 10^{-6} Y^3. \quad (15)$$

This ratio, according to [11], shows the best approximation accuracy of experimental data in comparison with other equations for water activity.

The difference between the model proposed in this paper and those described in [9-11] lies in the additional consideration of the change in the concentration of the solution due to the dissolution of the crystalline core in the form:

$$Y = 100 \cdot \frac{(n_2 - n_{2k}) \rho_2 v_2}{(n_2 - n_{2k}) \rho_2 v_2 + n_1 \rho_1 v_1}, \quad (16)$$

where ρ_1 and ρ_2 — density of water and solute matter, respectively. Thus, the expression for water activity will be a function of two variables $a_w(n_1, n_{2k})$.

As a result, the equation for evolution of the water molecules number in a particle takes the form:

$$\frac{dn_1}{dt} = \frac{4\pi r_* D_f p_n(T_\infty)}{k_b} \left(\frac{\varphi}{T_\infty} - \frac{a_w(n_1, n_{2k})}{T_*} \exp\left[\frac{LM_1}{R_g} \left(\frac{1}{T_\infty} - \frac{1}{T_*} \right) + \frac{2\sigma_1 v_1}{r_* k_b T_*} \right] \right), \quad (17)$$

where the particle radius is determined from the relation (11).

To close the equation (17), it is required to write down the relations for the temperature T_* and the number of the crystalline matter molecules in the particle n_{2k} . Assuming that the dissolution process of a crystalline matter is diffusion and depends on the concentration of the solution on the particle surface, the equation for the dissolution rate of a crystalline matter will be:

$$\frac{dn_{2k}}{dt} = \theta(n_1 - A_\varphi) \left\{ -4\pi D_d r_k \frac{N_a}{M_2} \left[(C_n - C_i) \theta(C_n - C_i) + (C_{pn} - C_i) \theta(C_i - C_{pn}) \right] \right\}, \quad (18)$$

$$r_k = \left(\frac{3v_2(n_{2k} + 1)}{4\pi} \right)^{1/3}, \quad C_i = \frac{M_2}{N_a} \frac{(n_2 - n_{2k})}{(n_1 v_1 + (n_2 - n_{2k}) v_2)},$$

where C_n , C_{pn} , C_i — mass concentration of saturated, supersaturated and solute matter on the surface of the undissolved particle core, N_a - Avogadro's number, D_d - diffusion coefficient of dissolved molecules in the solution, $\theta(x)$ - the Heaviside function, which allows us to “turn off” the dissolution of the crystal core

until an adsorption layer of the required capacity ($n_1 = A_\varphi$) is formed, as well as to “start” the dissolution process under the condition $C_i < C_n$ and crystallization when $C_i > C_{pn}$.

Since condensation is accompanied by the release of heat, and evaporation – by the intake of heat, the temperature of the particle T_* (it is assumed that the particle is heated uniformly) changes. In turn, due to thermal conductivity, heat exchange of the particle with the surrounding air occurs, during which the temperature of the particle tends to equalize with the ambient temperature, which is assumed to be constant T_∞ . As a result, the rate of particle temperature evolution is determined by the relation:

$$c_p m \frac{dT_*}{dt} = 4\pi r_* \varkappa (T_\infty - T_*) + L \frac{dm}{dt}, \quad (19)$$

where c_p — specific heat capacity of a particle, \varkappa — coefficient of thermal conductivity of humid air, L — specific heat of vaporization (condensation). Taking into account that the mass of the particle is $m = n_1 \rho_1 v_1 + n_2 \rho_2 v_2$, and the number of molecules of the dissolved substance is constant $n_2 = \text{const}$, the equation (19) can be rewritten as:

$$\frac{dT_*}{dt} = \frac{1}{c_p (n_1 \rho_1 v_1 + n_2 \rho_2 v_2)} \left[4\pi r_* \varkappa (T_\infty - T_*) + L \rho_1 v_1 \frac{dn_1}{dt} \right]. \quad (20)$$

Since the diffusion equations are applicable to the description of processes on a scale that is significantly longer than the mean free path of water molecules in air λ (which is under normal atmospheric conditions $\lambda \cong 10^{-1} \mu\text{m}$), then for particles with a radius of about 1 μm or less (Knudsen number $\text{Kn} \cong 10^{-1}$), the diffusion approximation cannot be considered sufficiently rigorous. Therefore, the equations of condensations particle growth and heat diffusion (17), (18) and (20) are corrected by changing the diffusion and thermal conductivity coefficients [8]:

$$D_f^* = D_f \left[\frac{1}{1 + \delta_c \lambda / r_*} + \frac{D_f}{r_* \alpha_c \sqrt{R_g T_*} / (2\pi M_1)} \right]^{-1}, \quad \varkappa^* = \varkappa \left[\frac{1}{1 + \delta_c \lambda / r_*} + \frac{\varkappa}{r_* \alpha_t \rho_{\text{air}} c_{p,\text{air}} \sqrt{R_g T_*} / (2\pi M_{\text{air}})} \right]^{-1}. \quad (21)$$

In this work, as well as in the article [9], the mass and temperature coefficients of accommodation $\alpha_c = 1$ and $\alpha_t = 0,3$, $\delta_c = \delta_t = 2/3$, ρ_{air} , $c_{p,\text{air}}$ - density and specific heat of humid air.

3. Hygroscopic particle size evolution model for sodium chloride

The equations (17), (18) and (20) with respect to the variables n_1 , n_{2k} and T_* , together with the initial conditions (4)-(9), allow us to describe the evolution of the size and temperature of a particle in the processes of its dissolution and transformation into a drop, increase in size due to vapor condensation and evaporation of the drop, as well as its crystallization. The system of equations was solved sequentially using the numerical Euler method. It should be noted that this numerical method is sensitive to the time step used; therefore, in the calculations, the time step was split until a convergent solution was reached.

The notations introduced into the model and the values of the parameters used in the calculations (taken from the addendum to the article [11]) are presented in Table 1.

Table 1. Values of the parameters used in the calculations.

Vapor diffusion coefficient	Notations	Units	Values/equations
Diffusion coefficient of NaCl in solution	M_2	kg/mol	$58,45 \times 10^{-3}$
Air density	ρ_2	kg/m ³	2165
Specific heat capacity of air at 295,15K	v_2	m ³	$M_2 / (\rho_2 N_a) = 4,487 \times 10^{-29}$

Thermal conductivity of dry air	d_1	m	$\approx 3 \times 10^{-10}$
Thermal conductivity of saturated vapor	M_1	kg/mol	18×10^{-3}
Thermal conductivity of humid air	ρ_1	kg/m ³	993,36
Specific heat of vaporization/condensation	v_1	m ³	$M_1/(\rho_1 N_a) = 3,012 \times 10^{-29}$
Vapor diffusion coefficient	σ_1	N/m	73×10^{-3}
Diffusion coefficient of NaCl in solution	c_p	J/(K kg)	4179 (in the calculation it was assumed equal to the specific heat capacity of water)
Air density	C_{pn}^n, C_{pn}^m	kg/m ³	306,914, 460,371
Specific heat capacity of air at 295,15K	$p_n(T)$	Pa	$2,3388 \times 10^3$ for $T = 293$ K; $3,3629 \times 10^3$ for $T = 299,15$ K; $9,5898 \times 10^3$ for $T = 318$ K
Thermal conductivity of dry air	D_f	m ² /s	22×10^{-6}
Thermal conductivity of saturated vapor	D_d	m ² /s	3×10^{-10}
Thermal conductivity of humid air	ρ_{air}	kg/m ³	1,18
Specific heat of vaporization/condensation	$c_{p,air}$	J/(K kg)	1005
Vapor diffusion coefficient	\varkappa_a	J/(K s m)	$(7,3172 \times 10^{-5})T_\infty + 4,1147 \times 10^{-3}$
Diffusion coefficient of NaCl in solution	\varkappa_v	J/(K s m)	$(1,663 \times 10^{-7})T_\infty^2 - (3,528 \times 10^{-5})T_\infty + 1,484 \times 10^{-2}$
Air density	\varkappa	J/(K s m)	$(\varkappa_a + x_v(0,8536\varkappa_v - \varkappa_a))/(1 - 0,1464x_v)$, where $x_v = 0,0185$
Specific heat capacity of air at 295,15K	L	J/kg	$10^3(2500,8 - 2,36(T_\infty - 273,15) + 0,0016(T_\infty - 273,15)^2 - 0,00006(T_\infty - 273,15)^3)$

Fig. 3 shows the model-calculated time evolution of the water molecules number n_1 (solid line) and of the undissolved sodium chloride molecules number n_{2k} (dashed line) in the particle at various relative humidity values of the ambient air: $\varphi = 0,35$ (below the crystallization point ERH) and $\varphi = 0,9$ (above the dissolution point DRH) at $T_\infty = 293$ K. The study was carried out as for the particle, which was initially absolutely dry $n_{10} = 0$ with a radius $r_0 = 1 \mu\text{m}$ (which corresponds to the total amount of the dissolved matter in the particle $n_2 = 9,3 \times 10^{10}$), as well as for the particle, which was completely dissolved $n_{10} = 0,91n$ at the initial moment, with a radius $r_0 = 1,69 \mu\text{m}$ (which also corresponds to $n_2 = 9,3 \times 10^{10}$).

It can be seen from Fig. 3a that for a particle that is initially in a dry state, an adsorption layer is first formed without the dissolution of the nucleus. When the layer capacity reaches its critical value for a given relative humidity, the particle begins to dissolve, however, due to the low humidity of the surrounding air, the influx of water molecules into the particle is not carried out, so the dissolution process stops. When a dry particle is placed in the air with high relative humidity, (Fig. 3c) at the initial stage $t < 1 \times 10^{-6}$ s the adsorption process is also observed, followed by complete dissolution of sodium chloride and a gradual increase in the number of water molecules in the droplet until an equilibrium state is reached.

If a completely dissolved particle is placed in the air with low relative humidity (Fig. 3e), at the first stage, water molecules intensively evaporate from the surface of the droplet, which causes an increase in the concentration of the solution inside the droplet. When the solution in the drop becomes supersaturated, along with the evaporation of the particle, the process of its crystallization begins, which continues until the steady state. The behavior of a dissolved particle in the air with a relative humidity above DRH corresponds to the process of droplet condensation (Fig. 3g).

As follows from Fig. 3*b, d, h*, the particle heats up during its growth due to the condensation of water molecules. The maximum increase in temperature occurs, when the concentration of the salt solution on the surface of the particle is minimal and, as a result, the process of water condensation is most intense. As the concentration goes down, the heating of the particle due to condensation decreases and the process of heat conduction becomes predominant. It leads to the removal of heat from the particle.

During the drying process (Fig. 3*f*), at first the temperature of the particle decreases sharply due to the intensive evaporation of water molecules from the surface of the particle. As the water concentration in the drop decreases, the heat conduction process becomes predominant, which leads to gradual heating of the drop. However, when the solution concentration becomes equal to the supersaturation concentration and the crystallization process begins, the particle temperature decreases again. After crystallization is completed, the temperature of the particle rises to the temperature of the air surrounding it due to thermal conductivity.

Fig. 3 shows that the equilibrium time for the particle size varies from 10^{-6} s (Fig. 3*a*) to 10^{-1} s (Fig. 3*c, e, g*) and depends on how much its initial state differed from the equilibrium.

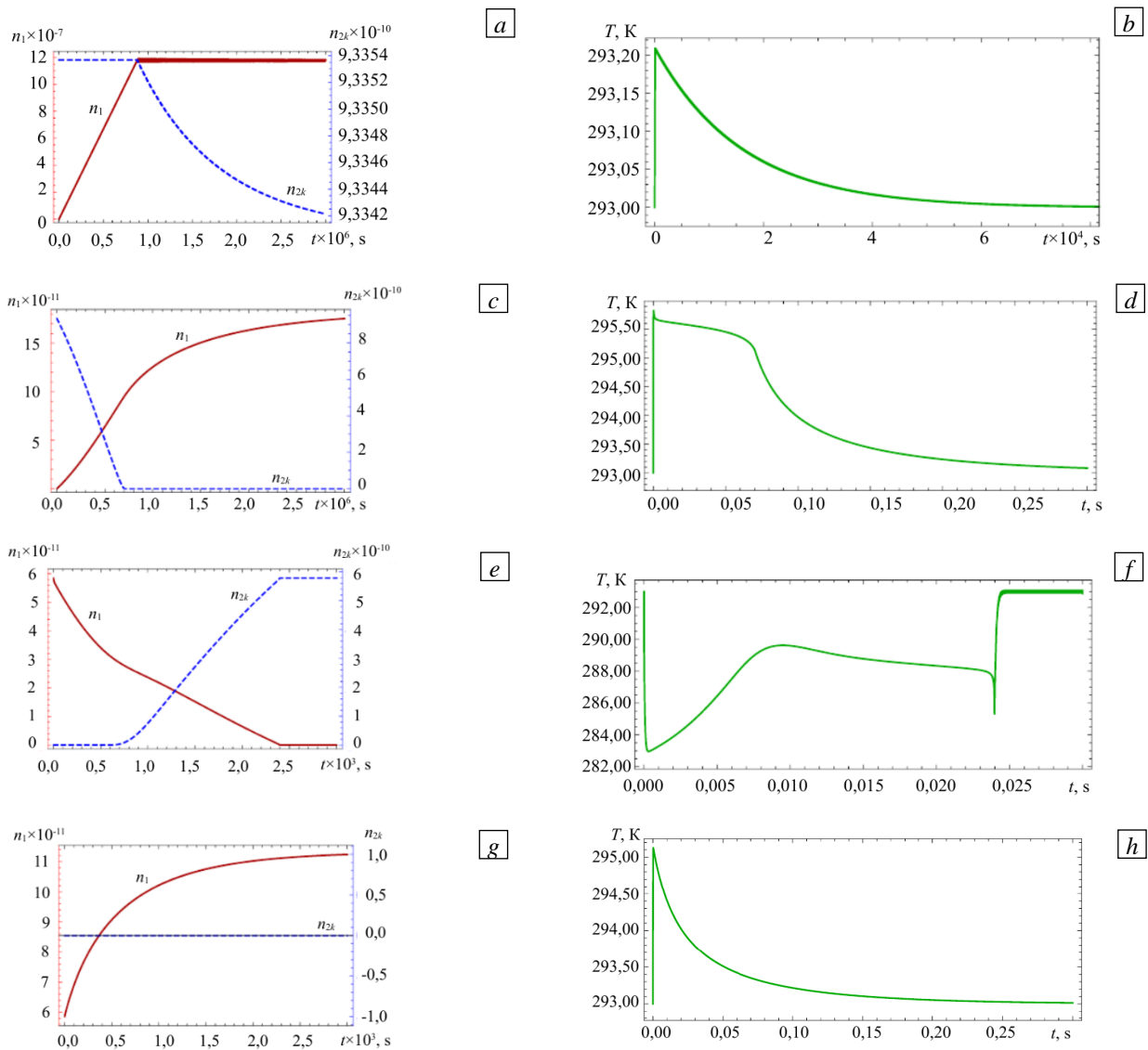


Fig. 3. Time evolution of the water molecules number n_1 (solid line), of undissolved sodium chloride molecules number n_{2k} (dashed line), and particle temperature for different values of the relative humidity of the ambient air and the initial mole fraction of water in the particle:

$\varphi = 0,35$, $n_{10} = 0$ (a, b); $\varphi = 0,9$, $n_{10} = 0$ (c, d); $\varphi = 0,35$, $n_{10} = 0,91n$ (e, f); $\varphi = 0,9$, $n_{10} = 0,91n$ (g, h).

To determine the validity of the transition from the equation (1) to (2), used in most models based on the modification of the Maxwell equation, we will evaluate the change in particle density during the process of dissolution. The calculations were carried out for an initially dry particle $n_{10} = 0$ with a diameter of 1 μm ,

which was placed in humid air. The simulation results for two values of relative humidity $\varphi = 0,8$ and $\varphi = 0,99$ are presented in Table 2 and in Fig. 4. The table shows the density values at the moment of complete dissolution of the crystalline core (droplet formation) ρ_i , the minimum particle density ρ_{\min} , which is achieved in the equilibrium state, as well as the proportion of density reduction relative to the initial state ρ_0 and the dissolved state ρ_i .

According to the results, there is a significant change in the particle density relative to the initial value ρ_0 , regardless of the relative humidity of the air. If relation (2) is used only to describe the dissolution of a drop (i.e., after the vertical dashed line in Fig. 4), then the change in density relative to the density of the drop at the moment when the particle begins to dissolve ρ_i will vary from 1,4% at a relative air humidity close to the hygroscopic point up to 11,6% at $\varphi = 0,99$.

Table 2. Evolution of particle density during dissolution

$\varphi \times 100$, %	$\rho_i, \text{kg/m}^3$	$\rho_{\min}, \text{kg/m}^3$	$\frac{\rho_0 - \rho_{\min}}{\rho_0} \times 100$, %	$\frac{\rho_i - \rho_{\min}}{\rho_i} \times 100$, %
80	1152	1136	47,5	1,4
99	1136	1004	53,6	11,6

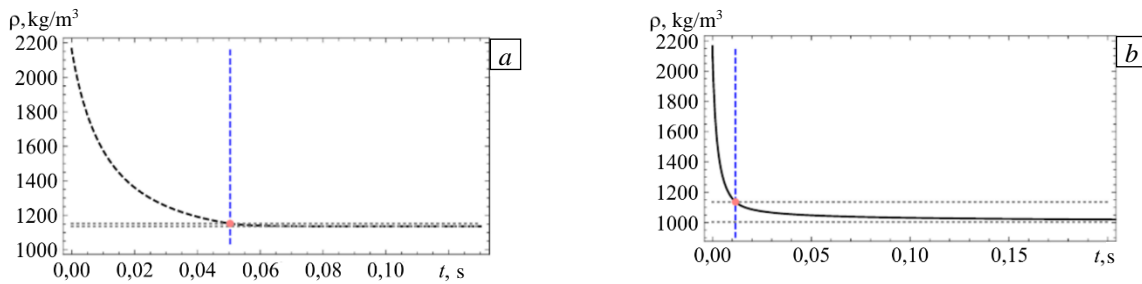


Fig. 4. Evolution of particle density in the process of hygroscopic growth at $r_0 = 0,5 \mu\text{m}$ and $T_* = 293 \text{K}$, $n_{10} = 0$, and $\rho_0 = 2165 \text{kg/m}^3$ different relative air humidity: (a) - $\varphi = 0,8$; (b) - $\varphi = 0,99$. The vertical dashed line separates two stages: the dissolution of a particle containing a crystalline core and the growth of a drop without a core.

4. Model verification

The model verification presented in the work was carried out by qualitative and quantitative comparison of its predictions with experimental data on the evolution of the particle size of sodium chloride in hydration and dehydration modes, as well as with the results of particle size measurements in the equilibrium state with an increase and decrease in the relative humidity of the air (with an absorption isotherm).

The model was tested in the hydration mode on the experimental data presented in [11]. In this work, a new system for measuring the size during droplet growth was developed, in which a preliminarily cleaned and dried aerosol particle is captured on a microscope glass coverslip placed in the air with controlled humidity and temperature. The particle growth process was recorded by a video camera. Fig. 5a shows data obtained by the described method on the growth of NaCl particles in the air with relative humidity $\varphi = 0,98$ at $T = 299,15 \text{K}$. It should be noted that the developed method does not allow measuring the three-dimensional structure of a dry particle, and, as a result, the initial size of the crystal particle is not known. In the simulation, the initial radius of the particle was adjusted until the standard error of the deviation of the model predictions from the experimental data over the 30-second test period was minimized. The best agreement between model predictions and experimental data was obtained for $2r_0 = 3,85 \mu\text{m}$ (see Fig. 5b).

Figure 6 shows the results of a linear regression analysis of the experimental and model values of the diameter both for the entire range of particle size measurements and only for the dissolution area of the crystalline core. As follows from the graphs, there is a good data correlation in both cases (the correlation coefficient r is close to 1, the linear regression equation deviates slightly from $y = x$). The Root Mean Square

Error (RMSE), which characterizes the difference between the predicted and experimental values, is $\approx 0,3\mu\text{m}$. Compared to similar data given in [11], the accuracy of predicting the hygroscopic growth of a particle by the proposed model increases. However, it should be taken into account that the author of the article [11] used the data of six series of experiments to study the accuracy.

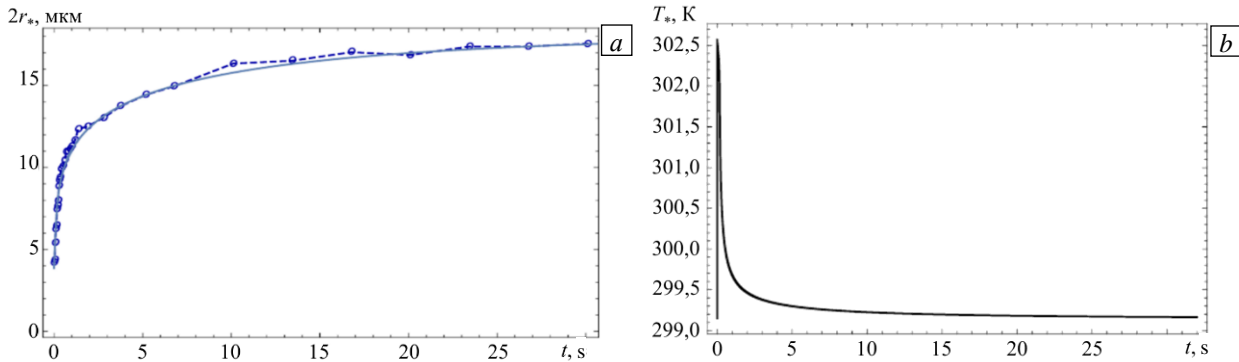


Fig. 5. Time evolution of: (a) - particle diameter calculated using the model (solid line) and measured in the experiment [11] (dots connected by a dashed line); (b) - particle temperature, at $\varphi = 0,98$, $T = 299,15\text{K}$, $2r_0 = 3,85\mu\text{m}$, $n_{10} = 0$.

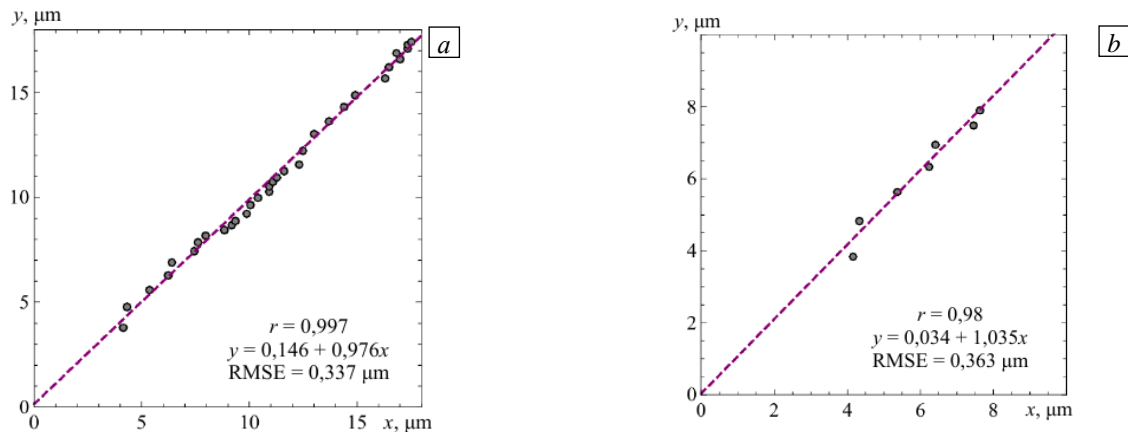


Fig. 6. Correlation between the diameters obtained in the experiment and the diameters predicted by the model, (a) - for all measurement time (from 0 to 30 s) and (b) - until the moment of dissolution of the crystalline.

Verification of the model in the dehydration mode (which connected with evaporation and crystallization) was carried out on the basis of the experimental and model data presented in [21]. In this work, the evaporation kinetics of NaCl droplets was measured using a device (CK-EDB) [22], which makes it possible to place generated and precharged aerosol droplets at the center of an electrodynamic field created by applying an alternating field between two sets of concentric cylindrical electrodes. The radius of isotropic droplets in dry air was determined using a laser. However, this method does not work when crystallization occurs, which upsets the particle isotropy, and the scattering pattern changes dramatically. Fig. 6 shows the results of measuring the particle size in the dehydration mode, obtained by the method described above. The experiments were carried out at controlled air temperatures of 293 K and 318 K for droplets with different initial mass fraction of solute (MFS). To convert to the mole fraction of water, the ratio was used:

$$x_1 = \frac{n_1}{n} = \left[1 + \frac{\text{MFS}M_1}{(100 - \text{MFS})M_2} \right]^{-1}. \quad (22)$$

The results of calculating the radius of a particle in the process of its evaporation and crystallization using the proposed model with parameters corresponding to the experimental conditions are shown in Fig. 7 together with experimental data and forecasts of the model used in [21]. It follows from the graphs that there is a fairly good agreement between the predictions of the model and experimental data in the area of particle evaporation,

however, the proposed model incorrectly predicts the onset of crystallization (vertical dashed line) at $T_\infty = 318$ K.

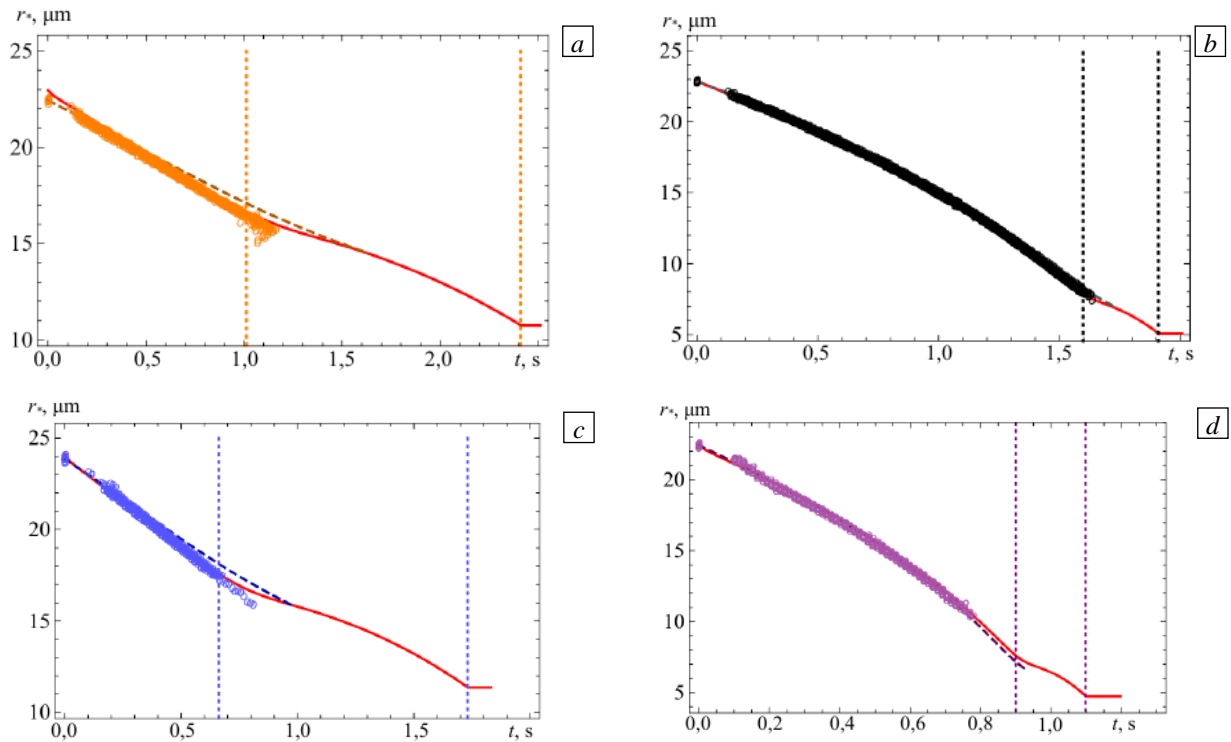


Fig. 7. Evolution of the radius of a NaCl drop in dry air $\varphi = 0\%$ for various ambient temperatures T_∞ and initial mass fractions of NaCl in a drop: obtained in the experiment (points « \circ »); calculated on the basis of the model proposed in [21] (dashed line); and using the model presented in this paper (solid line): MFS = 20% , $T_\infty = 293$ K, $r_0 = 22,95$ μm (a); MFS = 2,333% , $T_\infty = 293$ K, $r_0 = 22,95$ μm (b); MFS = 20,2% , $T_\infty = 318$ K $r_0 = 24,14$ μm (c); MFS = 2% , $T_\infty = 318$ K, $r_0 = 22,55$ μm (d). The vertical lines correspond to the start and end times of crystallization.

Table 3. Estimates of the accuracy of calculating the hygroscopic size reduction of sodium chloride particles.

Experiment conditions	RMSE, μm	Regression equation	R^2	$r = \sqrt{R^2}$
Model predictions from [21]				
MFS = 20% , $T_\infty = 293$ K	0,452	$y = 2,85 + 0,868x$	0,997	0,998
MFS = 2,333% , $T_\infty = 293$ K	0,279	$y = 0,665 + 0,973x$	0,999	0,999
MFS = 20,2% , $T_\infty = 318$ K	0,509	$y = 3,195 + 0,862x$	0,995	0,997
MFS = 2% , $T_\infty = 318$ K	0,289	$y = 0,327 + 0,995x$	0,997	0,998
Predictions of the proposed model				
MFS = 20% , $T_\infty = 293$ K	0,198	$y = 0,088 + 1,004x$	0,996	0,998
MFS = 2,333% , $T_\infty = 293$ K	0,138	$y = -0,238 + 1,009x$	0,999	0,999
MFS = 20,2% , $T_\infty = 318$ K	0,154	$y = 0,757 + 0,961x$	0,992	0,996
MFS = 2% , $T_\infty = 318$ K	0,170	$y = 0,458 + 0,976x$	0,998	0,999

Quantitative estimates of the error are given in Table 3. For convenience of comparison, similar data were also obtained for the model from [21]. As follows from the table, for the model under consideration, the standard deviations (RMSE) of the experimental and model data decrease for all considered test modes, and the linear regression curve noticeably approaches a straight line $y = x$.

Fig. 8 compares the absorption isotherms for NaCl aerosol particles predicted by the model proposed in this paper (solid lines with «▲» and «▼») and experimentally obtained in [23] («×» and «○»). The solid line with «▲» and the markers «○» correspond to the particle, which for each fixed value of relative humidity φ is initially dry, it is identical to the hydration mode, i.e. the gradual increase in the relative humidity of the air. The line with «▼» and the markers «×» are built for the initially dissolved particle, i.e. corresponds to the dehydration mode, i.e. the decrease of the relative humidity. As follows from the Figure, the model proposed in the work describes the experimentally observed hysteresis of the hygroscopic properties of NaCl particles, and also predicts the relative humidity of the phase transitions for dissolution and crystallization. It should be

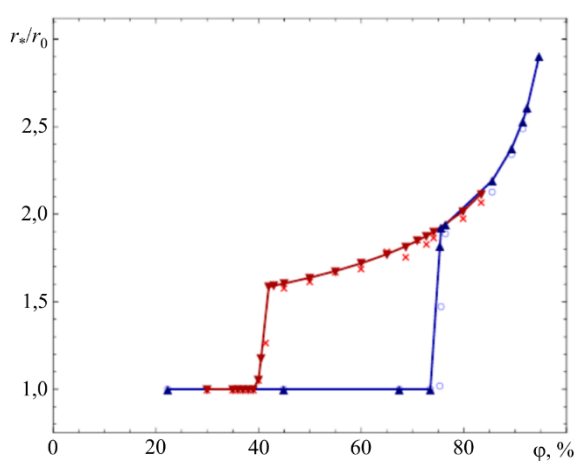


Fig. 8. Absorption isotherm for NaCl 1.

noted that, according to this model, in the mode of increasing relative humidity at $\varphi < DRH$, the particle is in a quasi-stationary state, which looks like a cyclic change in the processes of water condensation on the particle surface and its evaporation, and the number of water molecules in the particle fluctuates around the average value. This behavior can be explained by the fact that the water activity depends not only on the number of water molecules in the particle, but also on the amount of solute matter (NaCl). The phase transition in the evaporation mode is directly determined by the value of the supersaturation concentration C_{pm} , exceeding of which, due to the evaporation of water from the particle surface, leads to crystallization of the matter.

A quantitative estimate of the calculation error is given in Table 4. The main reason for the decrease in the prediction accuracy of the absorption isotherm is due to the fact that the DRH point predicted by the proposed model is slightly lower than the experimental value.

Table 4. Estimates of the calculation accuracy the absorption isotherm for a NaCl particle.

Experiment mode	RMSE, μm	Regression equation	R^2	$r = \sqrt{R^2}$
Increase φ	0,279	$y = 0,294 + 0,902x$	0,854	0,924
Decrease φ	0,055	$y = -0,028 + 1,04x$	0,983	0,991

5. Conclusion

A mathematical model has been constructed that makes it possible to describe the kinetics of the interaction of a water-soluble homogeneous and chemically neutral aerosol particle with humid air at all stages of its hygroscopic increase (decrease) in size. By taking into account the dependence of water activity on the concentration of the dissolved part of the particle and introducing an additional equation for the evolution of the undissolved core, in contrast to [11], it was possible to avoid artificial separation of the stages of dissolution of a particle with and without an undissolved core.

Based on the proposed model, the simulation of various scenarios for the particle size evolution depending on its initial dissolution degree and the relative humidity was carried out. It is shown that the predictions of the proposed model are qualitatively and quantitatively consistent with the experimental data on the evolution of the NaCl particle size in the hydration and dehydration modes, as well as with the results of particle size measurements in the equilibrium state with increasing and decreasing relative air humidity.

An estimate was made of the change in the density of a particle that is initially in a dry state. It has been established that during the hygroscopic growth of a particle in the air with high relative humidity (0,99), the change in density exceeds 10%, which must be taken into account when transforming the equation (1) to (2) in models based on the modification of the Maxwell equation.

The developed model can be useful for creating a complex mathematical model of coagulation and sedimentation of dust aerosol particles, taking into account the hygroscopic increase (decrease) in the size of particles.

Acknowledgments. The study was supported by the Russian Foundation for Basic Research (project № 20-45-596020) and under the assignment of the Ministry of Science and Higher Education of Russia (subject № 121031700169-1).

References

1. Tereshchenko A. *Gigroskopichnost' i slēzhivayemost' rastvorimykh veshchestv* [Hygroscopicity and traceability of soluble substances]. Tomsk, Tomsk Polytechnic University, 2011. 77 p.
2. Mikhailov E., Vlasenko S., Niessner R., Pöschl U. Interaction of aerosol particles composed of protein and salts with water vapor: hygroscopic growth and microstructural rearrangement. *Atmos. Chem. Phys.*, 2004, vol. 4, pp. 323-350. <http://dx.doi.org/10.5194/acp-4-323-2004>
3. Köhler H. The nucleus in and the growth of hygroscopic droplets. *Trans. Faraday Soc.*, 1936, vol. 32, pp. 1152-1161. <http://dx.doi.org/10.1039/tf9363201152>
4. Vul'fson A. Termodinamika ravnesiya nasyshchennogo vodyanogo para nad poverkhnost'yu kapli pri nalichii v ney tverdogo rastvorimogo yadra [Thermodynamics of the equilibrium of saturated water vapor over the surface of a drop in the presence of a solid soluble core in it]. *Izv. RAN. Fizika atmosfery i okeana – Izvestiya, Atmospheric and Oceanic Physics*, 1998, vol. 34, no. 2, pp. 1-8.
5. Vul'fson A. Usloviya ustoychivosti plenki nasyshchennogo rastvora na tverdoy sfericheskoy chastitse rastvoryayemogo veshchestva [Stability conditions of a saturated solution film on a solid spherical particle of a solute]. *Zh. fiz. khimii – Russian Journal of Physical Chemistry*, 1997, vol. 71, no. 12, pp. 2128-2134.
6. Kulmala M., Kerminen V.-M., Anttila T., Laaksonen A., O'Dowd C.D. Organic aerosol formation via sulphate cluster activation. *J. Geophys. Res.*, 2004, vol. 109, D04205. <http://dx.doi.org/doi:10.1029/2003JD003961>
7. Vanhanen J., Hyvarinen A.-P., Anttila T., Raatikainen T., Viisanen Y., Lihavainen H. Ternary solution of sodium chloride, succinic acid and water; surface tension and its influence on cloud droplet activation. *Atmos. Chem. Phys.*, 2008, vol. 8, pp. 4595-4604. <http://dx.doi.org/doi:10.5194/acp-8-4595-2008>
8. Pruppacher H.R., Klett J.D. *Microphysics of clouds and precipitation*. Springer, 2010. 954 p. <http://dx.doi.org/10.1007/978-0-306-48100-0>
9. Broday D.M., Georgopoulos P.G. Growth and deposition of hygroscopic particulate matter in the human lungs. *Aerosol Sci. Tech.*, 2001, vol. 34, pp. 144-159. <https://doi.org/10.1080/02786820118725>
10. Xie X., Li Y., Chwang A.T.Y., Ho P.L., Seto W.H. How far droplets can move in indoor environments – revisiting the Wells evaporation–falling curve. *Indoor Air*, 2007, vol. 17, pp. 211-225. <https://doi.org/10.1111/j.1600-0668.2007.00469.x>
11. O'Shaughnessy P.T., LeBlanc L., Pratt A., Altmaier R., Rajaraman P.K., Walenga R., Lin C.-L. Assessment and validation of a hygroscopic growth model with different water activity estimation methods. *Aerosol Sci. Tech.*, 2020, vol. 54, pp. 1169-1182. <https://doi.org/10.1080/02786826.2020.1763247>
12. Pöschl U., Rudich Y., Ammann M. Kinetic model framework for aerosol and cloud surface chemistry and gas-particle interactions – Part 1: General equations, parameters, and terminology. *Atmos. Chem. Phys.*, 2007, vol. 7, pp. 5989-6023. <https://doi.org/10.5194/ACP-7-5989-2007>
13. Shiraiwa M., Pfrang C., Pöschl U. Kinetic multi-layer model of aerosol surface and bulk chemistry (KM-SUB): the influence of interfacial transport and bulk diffusion on the oxidation of oleic acid by ozone. *Atmos. Chem. Phys.*, 2010, vol. 10, pp. 3673-3691. <https://doi.org/10.5194/acp-10-3673-2010>
14. Shiraiwa M., Pfrang C., Koop T., Pöschl U. Kinetic multi-layer model of gas-particle interactions in aerosols and clouds (KM-GAP): linking condensation, evaporation and chemical reactions of organics, oxidants and water. *Atmos. Chem. Phys.*, 2012, vol. 12, pp. 2777-2794. <https://doi.org/10.5194/acp-12-2777-2012>
15. Semeniuk K., Dastoor A. Current state of atmospheric aerosol thermodynamics and mass transfer modeling: A review. *Atmosphere*, 2020, vol. 11, 156. <http://doi.org/10.3390/atmos11020156>
16. Fridrichsberg D. *Kurs kolloidnoy khimii* [Colloidal chemistry course]. Leningrad, Khimiya, 1984. 368 p.
17. Harmon C.W., Grimm R.L., McIntire T.M., Peterson M.D., Njegic B., Angel V.M., Alshawa A., Underwood J.S., Tobias D.J., Benny Gerber R., Gordon M.S., Hemminger J.C., Nizkorodov S.A. Hygroscopic growth and deliquescence of NaCl nanoparticles mixed with surfactant SDS. *J. Phys. Chem.*, 2010, vol. 114, pp. 2435-2449. <https://doi.org/10.1021/jp909661q>

18. Robinson R., Stokes R. *Electrolyte solutions: The measurement and interpretation of conductance, chemical potential and diffusion in solutions of simple electrolytes*. London, Butterworths, 1970. 571 p.
19. Tang I.N., Munkelwitz H.R. Water activities, densities, and refractive indices of aqueous sulfates and sodium nitrate droplets of atmospheric importance. *J. Geophys. Res.*, 1994, vol. 99, pp. 18801-18808. <https://doi.org/10.1029/94JD01345>
20. Clegg S.L., Brimblecombe P., Wexler A.S. Thermodynamic model of the system $\text{H}^+ - \text{NH}_4^+ - \text{Na}^+ - \text{SO}_4^{2-} - \text{NO}_3^- - \text{Cl}^- - \text{H}_2\text{O}$ at 298.15 K. *J. Phys. Chem.*, 1998, vol. 102, pp. 2155-2171. <http://dx.doi.org/10.1021/jp973043j>
21. Robinson J.F., Gregson F.K.A., Miles R.E.H., Reid J.P., Royall C.P. Nucleation kinetics in drying sodium nitrate aerosols. <https://arxiv.org/abs/1911.06212>
22. Davies J.F., Haddrell A.E., Reid J.P. Time-resolved measurements of the evaporation of volatile components from single aerosol droplets. *Aerosol Sci. Tech.*, 2012, vol. 46, pp. 666-677. <https://doi.org/10.1080/02786826.2011.652750>
23. Tang I.N., Munkelwitz H.R., Davis J.G. Aerosol growth studies – II. Preparation and growth measurements of monodisperse salt aerosols. *J. Aerosol Sci.*, 1977, vol. 8, pp. 149-159. [https://doi.org/10.1016/0021-8502\(77\)90002-7](https://doi.org/10.1016/0021-8502(77)90002-7)

The paper was submitted 19.04.2021; approved after reviewing 02.11.2021; accepted for publication 03.12.2021